JOURNAL OF SOLID STATE CHEMISTRY 108, 366–370 (1994)

Reduced Molybdenum–Niobium Oxides:

II. Crystal Structure of $(Mo, Nb)_{13}O_{33}$

S. C. Chen and M. Greenblatt[1]

Department of Chemistry, Rutgers, The State University of New Jersey, Piscataway, NJ 08855-0939

Received March 19, 1993; in revised form May 27, 1993; accepted June 8, 1993

$(Mo, Nb)_{13}O_{33}$ crystallizes in the triclinic system, space group $P\bar{1}$ (No. 2). The unit cell dimensions are $a = 3.8194(4)$ Å, $b = 11.2898(7)$ Å, $c = 14.9764(9)$ Å, $\alpha = 94.039(5)°$, $\beta = 97.326(6)°$, $\gamma = 99.748(7)°$, $V = 628.47(9)$ Å^3, and $Z = 1$. The structure was refined to $R = 0.032$, $R_w = 0.036$, with 1460 observed reflections ($I > 3\sigma(I)$) and 186 variable parameters. The structure of $(Mo, Nb)_{13}O_{33}$ is related to the crystallographic shear structure of the $Nb_2O_{5-\delta}$ family and is built up from the $3 \times 4 \times \infty$ building blocks of the ReO_3-type MO_6 octahedra (M = Mo, Nb) and strings of edge-sharing MoO_4 tetrahedra running along [101]. The 3×4 ReO_3-type slabs at different heights along [101] are interconnected through corner sharing with the MoO_4 tetrahedra. $(Mo, Nb)_{13}O_{33}$ is an insulator at room temperature.

INTRODUCTION

Many transition metal oxide bronzes show metallic conduction that arises from partial filling of the conduction π^* band with strong d character (1). In the molybdenum bronzes, the Mo $4d$ (t_{2g}) orbitals overlap with the oxygen $p\pi$ orbitals of the MoO_6 octahedra to form bonding π and antibonding π^* bands. These π bonding orbitals are responsible for the possible formation of local Mo–O double bonds, which lead to distorted MoO_6 octahedra. Such distortion, however, can be partially relieved by the presence of electrons in the π^* antibonding orbitals, which open some of the Mo–O double bonds and result in a more regular octahedron. These considerations suggest that the conductive behavior of molybdenum bronzes are correlated to the Mo–O distances and therefore to the effective charges of the Mo atoms. Crystal structures are therefore needed in the understanding of the conduction properties of these compounds.

Despite the numerous examples of transition metal oxide bronzes of the type M_xO_y and $A_xM_yO_z$ (A is typically an alkali metal atom) (1–6), little is known about the reduced oxides of the type $A_nM_xM'_yO_z$, where M = Nb, Ta, and M' = Mo, W. We have previously reported two quaternary Mo–Nb bronzes: $K_{5.3}Mo_{9.2}Nb_{0.8}O_{30}$ with tetragonal tungsten bronze-type structure (7) and $K_2Mo_4Nb_3O_{20}$, which contains pentagonal columns composed of MO_7 and MO_6 (M = Mo, Nb) polyhedra (8). Here we report the crystal structure of another reduced Mo–Nb oxide—$(Mo, Nb)_{13}O_{33}$.

EXPERIMENTAL

Prior to use, K_2CO_3 (Aldrich, 99+%) was dried at 300°C for 1 hr, Nb_2O_5 (Alfa Product, 99.5%) was dried at 1100°C for 9 hr, and MoO_3 (Johnson Matthey, 99.95%) was dried at 550°C for 9 hr in air. K_2MoO_4 was prepared by the reaction of K_2CO_3 with a stoichiometric amount of MoO_3 in an alumina crucible at 550°C for 15 hr in air. Mo (Alfa Products, −100 mesh, 99.7%) was used as obtained without any further purification.

In a reaction aimed to prepare polycrystalline single-phase $K_{5.3}Mo_{9.2}Nb_{0.8}O_{30}$ (7), a mixture containing stoichiometric amounts of K_2MoO_4, MoO_3, Nb_2O_5, and Mo was thoroughly mixed, put in a platinum boat, and then sealed in a quartz tube under a dynamic vacuum. The reaction mixture was fired at 500°C overnight and then at 1100°C for another 5 days. Black, needle-shaped crystals of $(Mo, Nb)_{13}O_{33}$ grown in the flux were isolated from the matrix by alternate washes with hot, dilute K_2CO_3 (5% in weight) and HCl solutions.

A crystal having approximate dimensions of $0.03 \times 0.03 \times 0.24$ mm^3 was selected for both elemental analysis and single crystal X-ray crystallographic study. The qualitative elemental analysis on this single crystal with a scanning electron microscope (AMRAY 1400) indicated the presence of Mo and Nb with an approximate molar ratio of 3 : 10. Details of the X-ray crystallographic data of $(Mo, Nb)_{13}O_{33}$ are presented in Table 1. Lattice parameters and the orientation matrix for data collection were measured from 25 carefully centered reflections in the range 8° <

[1] To whom correspondence should be addressed.

0022-4596/94 $6.00

TABLE 1
Details of the X-Ray Crystallographic Data for (Mo, Nb)$_{13}O_{33}$[a]

Empirical formula	$Mo_{13}O_{33}$
Formula weight	1775.2
Crystal system	Triclinic
Space group	$P\bar{1}$ (No. 2)
a, Å	3.8194(4)
b, Å	11.2898(7)
c, Å	14.9764(9)
α, °	94.039(5)
β, °	97.326(6)
γ, °	99.748(7)
V, Å^3	628.47(9)
Z	1
Calculated density, g/cm^3	4.68
Crystal size, mm	0.03 × 0.03 × 0.24
μ(Mo$K\alpha$), cm^{-1}	62.2
Diffractometer	Enraf–Nonius CAD4
λ, Å, graphite-monochromated	0.71069
T, °C	20
2θ range, °	0–60
Scan mode	$\omega - 2\theta$
No. reflections collected	3000
No. observations ($I > 3\sigma(I)$)	1460
No. variables	186
Goodness-of-fit indicator[b]	1.02
Largest peak in final diffraction map, e^-/Å^3	0.926
Transmission coefficient (ψ-scan)	0.845–0.997
Correction factors (numerical)	0.773–1.087
R[c], R_w[d]	0.032, 0.036

[a] Data reported are based on the refined model of $Mo_{13}O_{33}$.
[b] Quality-of-fit = $[\Sigma\omega(|F_0| - |F_c|)^2/(N_{obs} - N_{parameters})]^{1/2}$.
[c] $R = \Sigma||F_0| - |F_c||/\Sigma|F_0|$.
[d] $R_w = [\Sigma\omega(|F_0| - |F_c|)^2/\Sigma\omega|F_0|^2]^{1/2}$; $\omega = 1/(\sigma^2|F_0|)$.

$2\theta < 37°$. Three standard reflections measured every 2 hr showed no apparent decay in intensity in the course of data collection. The intensity data were corrected for Lorentz-polarization effects. Because the MO_6 (M = Mo, Nb) octahedra are highly distorted, and because of the similarity of the scattering factors of Nb and Mo, the Nb and Mo atoms are indistinguishable in the structural refinement. The structure was thus refined with the model of $Mo_{13}O_{33}$. The linear absorption coefficient for Mo$K\alpha$ is 62.2 cm^{-1}, based on the $Mo_{13}O_{33}$ model. The empirical absorption correction based on ψ scans of three reflections was applied. The transmission factors were in the range 0.845–0.997. The reflection data were collected for the hemisphere (h, $\pm k$, $\pm l$).

The space group $P\bar{1}$ (No. 2) was chosen based on the statistical analysis of intensity distribution. The structure was solved by direct methods (SHELXS-86) (9) and refined on $|F|$ by using the full-matrix least-squares techniques in the MolEN program package (10). A θ-dependent absorption correction following the DIFABS procedure was applied to the isotropically refined structure (11). The maximum and minimum correction factors were 1.087 and 0.773, respectively. Based on 1460 reflections and 186 variable parameters, the structure was anisotropically refined to R = 0.032 and R_w = 0.036, with six of the seventeen oxygen atoms isotropically refined. The final electron density difference map was flat with a maximum of 0.926 e^-/Å^3 close to O (16). The final occupancy of $M(7)$ (M = Mo, Nb) atom is 0.523, resulting in an observed stoichiometry of (Mo, Nb)$_{13.46}O_{33}$. The stoichiometry of the title compound is then idealized as (Mo, Nb)$_{13}O_{33}$.

The final positional and isotropic thermal parameters of atoms are given in Table 2. Selected bond distances are listed in Table 3. The anisotropic thermal parameters of atoms (Table SI, 1 page), details of the interatomic bond distances (Table SII, 2 pages) and angles (Table SIII, 5 pages), and the observed and calculated structure factors (Table SIV, 10 pages) are available as supplementary materials.

RESULTS AND DISCUSSION

The polyhedral representation of the structure of (Mo, Nb)$_{13}O_{33}$ along the a axis is given in Fig. 1. The structure

TABLE 2
Final Positional Parameters and B_{eq}[a] for $M_{13}O_{33}$ (M = Mo, Nb)

Atom	x	y	z	B_{eq}, Å^2
$M(1)$	0.9654(4)	0.0470(1)	0.88120(8)	1.55(2)
$M(2)$	0.1747(3)	0.37686(9)	0.97353(7)	0.68(2)
$M(3)$	0.2493(3)	0.28381(9)	0.21403(7)	0.62(2)
$M(4)$	0.1112(3)	0.85897(9)	0.36269(7)	0.52(2)
$M(5)$	0.3223(2)	0.18857(9)	0.45620(6)	0.53(2)
$M(6)$	0.1022(2)	0.47214(8)	0.73161(7)	0.49(2)
$M(7)$	0.2504(5)	0.5000(2)	0.5000(1)	0.48(3)[b]
O(1)	0.459(2)	0.0491(8)	0.8707(6)	1.1(1)
O(2)	0.223(2)	0.0250(7)	0.4191(5)	0.7(1)
O(3)	0.145(2)	0.4373(7)	0.8485(5)	0.6(1)
O(4)	0.065(2)	0.5350(7)	0.5973(5)	0.7(1)
O(5)	0.003(2)	0.6807(7)	0.3234(5)	0.8(2)
O(6)	0.299(2)	0.2448(7)	0.3465(5)	0.6(1)
O(7)	0.076(2)	0.8996(8)	0.2505(5)	1.1(2)
O(8)	0.073(2)	0.2207(7)	0.9243(5)	1.0(2)
O(9)	0.223(2)	0.6730(7)	0.7693(5)	0.8(1)
O(10)	0.222(2)	0.3389(8)	0.0957(5)	0.9(1)
O(11)	0.148(2)	0.1271(6)	0.1756(5)	0.9(2)
O(12)	0.383(2)	0.1567(7)	0.6046(5)	0.5(1)[c]
O(13)	0.0	0.0	0.0	1.0(2)[c]
O(14)	0.444(2)	0.3712(7)	0.5173(5)	0.5(1)[c]
O(15)	0.155(2)	0.8068(6)	0.5074(5)	0.4(1)[c]
O(16)	0.376(2)	0.4777(7)	0.2690(5)	0.7(1)[c]
O(17)	0.294(2)	0.5767(6)	0.0196(4)	0.1(1)[c]

[a] $B_{eq} = 8\pi^2/3\ \Sigma U_{ij} a_i^* a_j^* \mathbf{a}_i \cdot \mathbf{a}_j$, where the temperature factors are defined as $\exp(-2\pi^2\ \Sigma h_i h_j a_i^* a_j^* U_{ij})$.
[b] The refined occupancy of $M(7)$ is 0.523.
[c] Atoms were refined isotropically.

TABLE 3
Selected Bond Distances (Å) for $M_{13}O_{33}$ (M = Mo, Nb)

$M(1)$–O(1)	1.93(1)	$M(4)$–O(12)	1.991(9)
$M(1)$–O(1)	1.91(1)	$M(4)$–O(12)	1.973(9)
$M(1)$–O(7)	2.10(1)	$M(4)$–O(15)	2.282(9)
$M(1)$–O(8)	1.98(1)	$M(5)$–O(2)	1.853(9)
$M(1)$–O(11)	2.041(9)	$M(5)$–O(6)	1.802(9)
$M(1)$–O(13)	1.890(2)	$M(5)$–O(12)	2.269(9)
$M(2)$–O(3)	2.038(9)	$M(5)$–O(14)	2.149(9)
$M(2)$–O(8)	1.822(9)	$M(5)$–O(15)	1.976(9)
$M(2)$–O(10)	1.904(9)	$M(5)$–O(15)	1.992(9)
$M(2)$–O(17)	2.267(8)	$M(6)$–O(3)	1.817(9)
$M(2)$–O(17)	1.961(9)	$M(6)$–O(4)	2.178(9)
$M(2)$–O(17)	1.995(9)	$M(6)$–O(5)	1.818(9)
$M(3)$–O(6)	2.058(9)	$M(6)$–O(9)	2.254(9)
$M(3)$–O(9)	1.986(9)	$M(6)$–O(16)	1.999(9)
$M(3)$–O(9)	1.972(9)	$M(6)$–O(16)	1.980(9)
$M(3)$–O(10)	1.919(9)	$M(7)$–O(4)	1.751(9)
$M(3)$–O(11)	1.785(9)	$M(7)$–O(4)	1.745(9)
$M(3)$–O(16)	2.24(1)	$M(7)$–O(14)	1.761(9)
$M(4)$–O(2)	1.958(9)	$M(7)$–O(14)	1.761(9)
$M(4)$–O(5)	2.02(1)	$M(7)$–$M(7)$	1.912(4)[a]
$M(4)$–O(7)	1.77(1)	$M(7)$–$M(7)$	1.906(4)[a]

[a] Distances between disordered $M(7)$ atoms.

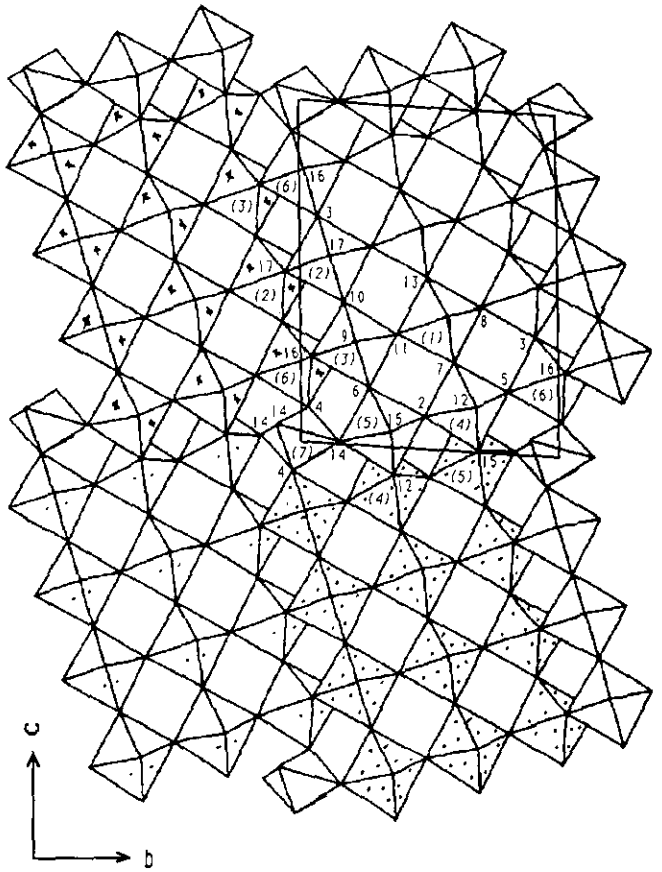

FIG. 1. Polyhedral represenation of the structure of $M_{13}O_{33}$ (M = Mo, Nb). The unit cell has been shifted by vectors of $0.5a$, $0.5b$, and $0.5c$ for the presentation of the 3 × 4 slab of ReO_3 type. The MO_6 and MO_4 polyhedra are labeled by italic numbers in parentheses. Other numerical labels are for the oxygen atoms. The different stipples in the ReO_3-type slabs represent different heights along [101].

of $(Mo, Nb)_{13}O_{33}$ consists of corner-sharing MO_6 octahedra and MO_4 tetrahedra (M = Mo, Nb). Twelve MO_6 octahedra share corners to form an ReO_3-type slab of three octahedra wide and four octahedra long (3 × 4). This slab is approximately on the (101) plane and intersects with the ac plane approximately along the diagonal direction, according to the atomic coordinates listed in Table 2. The 3 × 4 ReO_3-type slabs located at different heights along [101] are linked together via the corners of MO_4 tetrahedra running along the same direction. These ReO_3-type slabs edge share with each other at the peripheral octahedra along [101]. As shown in Fig. 2, the MO_4 tetrahedra are edge sharing along [101]. The oxygen atoms of the MO_4 tetrahedra are three coordinated and connect to the 3 × 4 slabs of ReO_3 type at different levels along [101].

The crystal structure of $(Mo, Nb)_{13}O_{33}$ is related to those of $P_xNb_9O_{25}$ (12, 13), VM_9O_{25} (M = Nb, Ta) (14), $Nb_{22}O_{54}$ (15) and H–Nb_2O_5 (16). The common structural features for these compounds are $m \times n$ ReO_3-type slabs of MO_6 (M = Nb, Ta) octahedra that are connected via MO_4 (M = P, V, Nb) tetrahedra by corner sharing. These ReO_3-type slabs linked via MO_4 (M = P, V, Nb) tetrahedra form layers perpendicular to the shortest crystallographic axis. The MO_4 (M = P, V, Nb) tetrahedra in these compounds edge share along the same axis. However, in $(Mo, Nb)_{13}O_{33}$, the 3 × 4 slabs are approximately perpendicular to [101] and the MO_4 tetrahedra edge share along the same

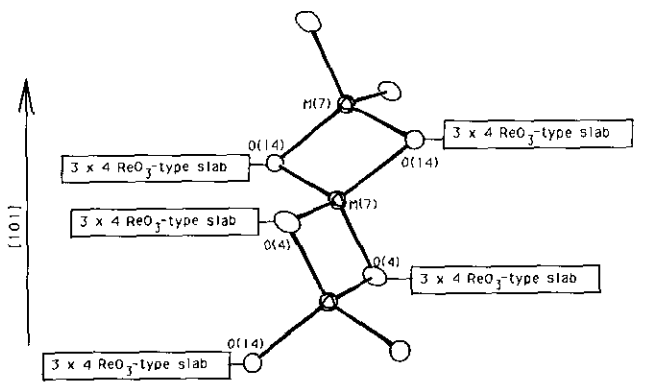

FIG. 2. ORTEP drawing (50% thermal ellipsoids) of a perspective view of the structure of $M_{13}O_{33}$ (M = Mo, Nb) showing the edge-sharing $M(7)O_4$ tetrahedra and their connections to the 3 × 4 ReO_3-type slabs along [101].

direction (Fig. 2). In contrast, the structure of molybdenum bronzes such as $K_{0.9}Mo_6O_{17}$ (17), $Li_{0.9}Mo_6O_{17}$ (18), $Cs(Mo_{0.95}W_{0.05})_7O_{21}$ (19), η-Mo_4O_{11}, and γ-Mo_4O_{11} (20) are built up from corner-sharing octahedra and tetrahedra with MoO_4 tetrahedra corner sharing along the shortest crystallographic axis.

Structures with infinite chains of edge-sharing MoO_4 tetrahedra are rare; the only other compound, besides (Mo, Nb)$_{13}O_{33}$ (to be discussed later), we could find with this feature is $MoTa_{12}O_{33}$ (21). Note that the infinite chains of edge-sharing WO_4 tetrahedra are also observed in $WNb_{12}O_{33}$ (22). Interestingly, these compounds crystallize in different space groups, regardless of their similar stoichiometry (identical metal-to-oxygen ratio) and analogous structural building units. The space group is *I2/m* for $MoTa_{12}O_{33}$, *C*2 for $WNb_{12}O_{33}$, and $P\bar{1}$ for (Mo, Nb)$_{13}O_{33}$.

As depicted in Fig. 1, there are six unique MO_6 (M = Mo, Nb) octahedra in the structure of (Mo, Nb)$_{13}O_{33}$. The $M(1)$ and its symmetry-related octahedra are located at the center of the 3 × 4 slab and corner share along the direction perpendicular to this ReO_3-type slab, i.e., [101]. The peripheral octahedra of the slabs edge share along the same direction: $M(2)$ octahedra with its symmetry-related ones, $M(3)$ with $M(6)$ octahedra, and $M(4)$ with $M(5)$ octahedra. The peripheral octahedra are much more distorted than the central ones, due to the local structural strains built up from edge sharing. This observation is supported by the M–O bond distances listed in Table 3. The $M(1)$–O distances of the central octahedron fall in the range 1.890(2)–2.10(1) Å (average 1.98 Å). The M–O distances of the peripheral octahedra are in the range 1.822(9)–2.267(8) Å (average 1.998 Å) for $M(2)$–O, 1.785(9)–2.24(1) Å (average 1.99 Å) for $M(3)$–O, 1.77(1)–2.282(9) Å (average 2.00 Å) for $M(4)$–O, 1.802(9)–2.269(9) Å (average 2.007 Å) for $M(5)$–O, and 1.818(9)–2.254(9) Å (average 2.008 Å) for $M(6)$–O. The M–O distances of the $M(7)O_4$ tetrahedron are between 1.745(9) and 1.761(9) Å, which fall in the range (1.704–1.83 Å) of the observed tetrahedral Mo–O distances (17–21), but are significantly longer than those (1.65–1.68 Å) of the edge-sharing NbO_4 tetrahedra (15, 16). Thus, we believe that the $M(7)$ atom in (Mo, Nb)$_{13}O_{33}$ is a molybdenum atom. Moreover, the observations of MoO_4 tetrahedron in $MoTa_{12}O_{33}$ (21) and WO_4 tetrahedron in $WNb_{12}O_{33}$ (22) further support this assignment. The partial occupancy (0.523) of the $M(7)$ atom and the extremely short $M(7)$–$M(7)$ distances (1.906(4) and 1.912(4) Å) suggest that the $M(7)$ atoms are disordered over the two tetrahedral sites of the edge-sharing bi-tetrahedral group and are never simultaneously occupied.

The relatively large isotropic temperature factor of the $M(1)$ (M = Mo, Nb) atom (Table 1) is due to its high anisotropy in the [100] direction. This anomaly may be explained by the central position of the $M(1)O_6$ octahedron in the ReO_3-type slab and the formation of a one-dimensional string of corner-sharing $M(1)O_6$ octahedra along [101]. The anisotropic temperature factors of the $M(1)$ atom are 0.0363(6) for U_{11}, 0.0102(4) for U_{22}, and 0.0107(4) for U_{33}. A similar behavior in the temperature factors of the metal atom in the central octahedron of the ReO_3-type slab was also observed in $P_xNb_9O_{25}$ (12, 13) and VM_9O_{25} (M = Nb, Ta) (14). A possible doubling of the a-axis could be another source of the thermal elongation of $M(1)$ along [100]. However, a 50 hr-exposure oscillation photograph taken with the a-axis as the rotation axis showed no evidence of superlattice along [100].

The qualitative room temperature resistivity measurement on a ~2-mm-long single crystal of (Mo, Nb)$_{13}O_{33}$, carried out by a two-probe technique with a Nanovoltmeter (Kethley model 180), indicated that the material is insulating with a room temperature resistivity in the order of 10^6 ohm · cm. A similar insulating behavior previously observed for $K_2Mo_4Nb_3O_{20}$ (8) was ascribed to localization due to potential electron traps created by the possible structural ordering of the Mo and Nb atoms.

In conclusion, we have structurally characterized a novel reduced molybdenum–niobium oxide with a three-dimensional shear structure derived from that of ReO_3 and closely related to that of Nb_2O_5. It is noteworthy that (Mo, Nb)$_{13}O_{33}$ is not isostructural with $MoTa_{12}O_{33}$ and $WNb_{12}O_{33}$, despite the similarity of their structural building blocks. (Mo, Nb)$_{13}O_{33}$ is an insulator, most likely due to localization of electrons in potential traps created by structural distortions and/or to the mixing of the Mo and Nb atoms.

ACKNOWLEDGMENTS

We thank Professor W. H. McCarroll for his critical reading of the manuscript. This work was supported by National Science Foundation Solid State Chemistry Grant DMR-90-19301.

REFERENCES

1. M. Greenblatt, *Chem. Rev.* **88,** 31 (1988).
2. E. Banks and A. Wold, "Preparative Inorganic Reactions" (W. L. Jolly, Ed.), Vol. 4, p. 237. Interscience, New York, 1968.
3. P. Hagenmuller, "Progress in Solid State Chemistry" (H. Reiss, Ed.), Vol. 5, p. 71. Pergamon, New York, 1971.
4. M. J. Sienko, "Non-Stoichiometric Compounds" (R. F. Gould, Ed.) p. 224, Advances in Chemistry Series. American Chemical Society, Washington, 1963.
5. P. G. Dickens and M. S. Whittingham, *Q. Rev., Chem. Soc.* **22,** 30 (1968).
6. A. Manthiram and J. Gopalakrishnan, *Rev. Inorg. Chem.* **6,** 1 (1984).
7. S. C. Chen and M. Greenblatt, *J. Solid State Chem.* **104,** 353 (1993).
8. S. C. Chen, B. Wang, and M. Greenblatt, *Inorg. Chem.* **32,** 4306 (1993).
9. G. M. Sheldrick, *in* "Crystallographic Computing 3" (G. M. Sheldrick, C. Kruger, and R. Goddar, Eds.), p. 175. Oxford Univ. Press, 1985.

10. C. K. Fair, "MolEN," Enraf–Nonius, Delft Instruments X-Ray Diffraction B. V., Rontgenweg 1, 2624 BD Delft, The Netherlands, 1990.
11. N. Walker and D. Stuart, *Acta Crystallogr., Sect. A* **39,** 158 (1983).
12. R. S. Roth and A. D. Wadsley, *Acta Crystallogr.* **18,** 643 (1965).
13. J. Xu, S. C. Chen, K. V. Ramanujachary, and M. Greenblatt, *Inorg. Chem.*, in press.
14. M. T. Casais, E. Gutierrez-Puebla, M. A. Monge, I. Rasines, and C. Ruiz-Valero, *J. Solid State Chem.* **102,** 261 (1993).
15. R. Norin, M. Carlsson, and B. Elgquist, *Acta Chem. Scand.* **20,** 2892 (1966).
16. B. M. Gatehouse and A. D. Wadsley, *Acta Crystallogr.* **17,** 1545 (1964).
17. H. Vincent, M. Ghedira, J. Marcus, J. Mercier, and C. Schlenker, *J. Solid State Chem.* **47,** 113 (1983).
18. M. Onoda, K. Toriumi, Y. Matsuda, and M. Sato, *J. Solid State Chem.* **66,** 163 (1987).
19. M. Zocchi, L. Depero, and F. Zocchi, *J. Solid State Chem.* **92,** 18 (1991).
20. L. Kihlborg, *Ark. Kemi* **21,** 365 (1963).
21. N. A. Yamnova, D. Yu. Pushcharovskii, L.I.Leonyuk, and A. V. Bogdanova, *Sov. Phys. Crystallogr. Engl. Transl.* **34**(2), 176 (1989).
22. R. S. Roth and A. D. Wadsley, *Acta Crystallogr.* **19,** 32 (1965).